



Characteristic equation development for double slope solar distiller unit augmented with N identical parabolic concentrator integrated evacuated tubular collectors

Sanjeev Kumar Sharma^a, Ashis Mallick^a, Sanjay K. Gupta^b, Navneet Kumar^c,
Desh Bandhu Singh^{d,*}, G.N. Tiwari^{e,f}

^aDepartment of Mechanical Engineering, Indian Institute of Technology (ISM) Dhanbad, Jharkhand, India, emails: sksharma6@amity.edu (S.K. Sharma), mal123_us@yahoo.com (A. Mallick)

^bDepartment of Civil Engineering, Indian Institute of Technology (BHU), Varanasi, Uttar Pradesh, India, email: skgupta.civ@iitbhu.ac.in

^cGalgotias College of Engineering and Technology, Plot No 1, Knowledge Park II, Greater Noida, UP, India, email: navneet.kumar@galgotiacollege.edu

^dMechanical Engineering Department, Graphic Era (Deemed to be University), Bell Road, Clement Town, Dehradun – 248002, Uttarakhand, India, email: dbsiit76@gmail.com

^eBag Energy Research Society (BERS), SODHA BERS COMPLEX, Plot No. 51, Mahamana Nagar, Karaudi, Varanasi, UP, 22 10 05, India

^fResearch and Development Cell, Shri Ramswaroop Memorial University (SRMU), Lucknow-Dewa Road, (UP), 226028, India, email: gntiwari@ces.iitd.ernet.in

Received 11 May 2019; Accepted 22 December 2019

ABSTRACT

This paper communicates the analytical equation development for double slope solar still coupled with a number of alike parabolic concentrator integrated evacuated tubular collector (NPCETCDS) which is also valid for evacuated tubular collector integrated double slope solar distiller unit (NETCDS) as well as passive double slope solar distiller unit (PDS). The developed equation is similar to Hottel-Whillier-Bliss equation which was developed for flat plate collector. The analytical equation development for NPCETCDS involves the writing of equations for its different components on the ground of equating net energy input to net energy output. The results obtained for the proposed NPCETCDS have been compared with results of NETCDS and PDS. It has been concluded that the average value of instantaneous efficiency for NPCETCDS is higher by 46.18% and 56.99%; and daily exergy is higher by 81.17% and 92.25% than the corresponding values for NETCDS and PDS for the same basin area in that order.

Keywords: Parabolic concentrator integrated evacuated tubular collector; Double slope solar still; Analytical equation

1. Introduction

The analytical equation development for an active double slope solar desalination unit can present one of the best considerations for assuaging the shortage of fresh water in the developing country as it is based on clean energy unlike conventional desalination unit which requires electrical

energy for its working. A number of theoretical and experimental studies exist in literature. The experimental investigation of basin type active solar desalination system in forced mode was presented for the first time by Rai and Tiwari [1]. In their investigation, it was concluded that the production of fresh water on daily basis for the basin type active solar desalination system consisting of one flat

* Corresponding author.

plate collector and working under dynamic mode was 24% greater than the daily production of potable water for the conventional solar desalination system. The higher output was obtained in the case of active solar desalination system due to the fact that additional heat using solar collector was supplied to the basin of solar still which resulted in higher rise in temperature of water in active system as compared with conventional solar still. The active mode of operation for solar desalination system involves the supply of heat to the basin by some external means such as integrating some type of collectors either directly or indirectly keeping heat exchanger in the basin and connecting the heat exchanger with the collector so that heat exchanger is in closed loop with collector. The objective of allowing the operation of solar desalination system in dynamic mode is to overcome the shortcoming of low production of potable water by conventional solar desalination system so that the solar desalination system can be used on commercial level.

Dev and Tiwari [2] used experimental data of basin type single slope passive solar desalination unit to bring about linear and non linear characteristic equations. They concluded that these equations can be used for selecting the solar still before its manufacturing and installations. Dev et al. [3] reported the development of characteristic equation for basin type double slope solar desalination unit and concluded that characteristic curves of non-linear types were producing better results for performance analysis and thermal testing. Singh et al. [4] and Singh and Tiwari [5] reported the development of analytical characteristic equation for solar desalination unit of basin type coupled with N alike ETCs. This system was proposed because heat loss due to convection does not take place in the case of ETC as vacuum was present in between two glass surfaces. Due to less heat loss as compared with other collectors where heat loss takes place by convection as well as radiation, higher amount of heat could be added to the basin of solar still in the system reported by Singh et al. [4] and Singh and Tiwari [5] which resulted in better performance of the system. Gupta et al. [6] have reported the characteristic equation development for single slope solar desalination unit coupled compound parabolic concentrator collector having 100% coverage with PVT. They covered receiver surface fully while keeping the number of solar cells same to the number of solar cells in partially covered PVT collector because of better performance of fully covered PVT collector due to lower top loss and lower maintenance. Dev and Tiwari [7] analyzed single slope solar still coupled with ETCs through heater and concluded that the proposed system produced 48% higher yield as compared with conventional single slope solar desalination unit because of heat addition to the basin through heater. In the case of evacuated tubular collector, the heat loss through convection does not take place and hence higher amount of heat is added. In the system reported by Dev and Tiwari [7], ETCs were not directly coupled to the basin of solar still. ETCs were connected to solar heater and hot water from solar heater was allowed to flow to the basin. A detailed review of solar desalination unit integrated with various collectors can be seen in the study by Sathyamurthy et al. [8].

Singh et al. [9] performed thermal modeling of solar desalination unit integrated with evacuated tubes and

evaluated the performance parameters under natural circulation mode. They found the exergy efficiency of the proposed system in the range of 0.15%–8%. They also found that the integration of evacuated tubes resulted in higher temperature of water in the basin and hence higher yield was obtained. The higher temperature of water in the basin was found due to the absence of convective heat loss as vacuum was present in between two glass tubes. Sampathkumar et al. [10] performed experimental study of evacuated tubes integrated solar desalination unit and concluded that the production of fresh water by proposed system was 129% higher than the passive solar desalination unit of same basin area due to addition of heat by collector to the basin. Further, Kumar et al. [11] performed thermal modeling of evacuated tubes coupled with single slope solar desalination unit under forced mode of operation and revealed that the generation of fresh water per hour was higher for the proposed system as compared with similar system having same basin area and working in natural mode because of increased temperature of water kept in basin due to higher amount of heat addition in the case of forced mode of operation. Mosleh et al. [12] made experimental investigation of a desalination system consisting of parabolic trough collector, evacuated tube and heat pipe. They concluded that the rate of production was 0.27 kg/m² h when aluminum foils were used for transferring heat to heat pipe from evacuated tube.

Shafii et al. [13] studied the modified solar desalination system consisting of evacuated tubes and reported that the highest production of desalinated water took place when the tube was inclined at latitude of the place and the tube was filled with 80% of brackish water because of higher normal radiation received at this angle. Sharshir et al. [14] investigated hybrid solar desalination unit based on the concept of humidification and dehumidification and consisting of evacuated tubes. They reported the gain output ratio of proposed system as 50%. Bait and Si-Ameur [15] investigated the improvement in performance of conventional double slope solar desalination unit by integrating the conventional double slope solar desalination unit with tubular solar collector taking potable water output as the basis. They reported that the heat loss in tubular solar collector was less than the flat plate collector because heat loss took place due to radiation only in the case of evacuated tubes resulting in higher yield and efficiency for the proposed system. Further, Bait [16] performed the exergy and enviroeconomic analyses for the system proposed by Bait and Si-Ameur [15]. Issa and Chang [17] studied experimentally single slope solar desalination unit coupled with evacuated tubes in series-parallel combination and compared this active solar desalination unit with the passive solar desalination unit for the same basin area. The arrangement of tubes was in mixed mode, that is, some tubes were connected in series and some in parallel. They reported that the fresh water production for active solar desalination unit was 61.11% higher than passive solar desalination unit because of supplying heat by collector to the basin of active solar desalination unit. Singh and Tiwari [18] made the theoretical study of basin type solar desalination unit by integrating with series connected N alike ETCs taking energy, exergy and cost of distillate as basis under optimized condition. The system reported by Singh and Tiwari [18] was different from the system reported by Issa and Chang [17] in the sense that

all collectors were connected in series in the case of system reported by Singh and Tiwari [18]; whereas, collectors were connected in mixed mode in the case of system reported by Issa and Chang [17]. They concluded that the cost of producing fresh water was lowered by 15.19% for double slope active solar desalination unit than the single slope active solar distiller having similar geometry due to higher fresh water production in the case of double slope active solar distiller at 280 kg of water mass in basin. Singh and Al-Helal [19] made theoretical analysis for double slope solar desalination unit integrated with N alike evacuated tubular collectors on the basis of energy metrics and concluded that the proposed system presented the best performance taking life cycle conversion efficiency as basis followed by double slope solar desalination unit coupled with PVT flat plate collectors and PVT compound parabolic concentrator collectors. They studied different active solar distillation systems under optimum condition. Singh [20] reported the comparative study of single slope active solar distiller on the basis of energy metrics. They made the comparative study among conventional single slope solar still; single slope solar still integrated with (a) PVT flat plate collectors and (b) PVT compound parabolic concentrator collectors. The single slope solar still integrated with PVT flat plate collectors was found to perform better on the basis of life cycle conversion efficiency due to higher number of collectors under optimum condition. Further, Singh [21] performed the exergoeconomic and enviroeconomic analyses of ETC integrated double slope solar distiller and concluded that double slope solar distiller included with ETC performance better than double slope solar distiller integrated with N alike photovoltaic thermal compound parabolic concentrator collectors (PVTCPs).

Elshamy and El-Said [22], performed comparative study tubular solar still with semi-circular corrugated absorber on the basis of thermal, exergetic and economic analyses and concluded that the water cost of the tubular solar still with semi-circular corrugated surface was 20.77% less than tubular solar still with flat plate. It happened because rise in temperature of water in the case of solar still with semi-circular corrugated surface was higher as compared with solar still with flat plate. Kabeel and El-Said [23–25] reported the experimental study and validation of hybrid solar distiller unit consisting of humidification and dehumidification units and solar air–water heater and concluded that the maximum daily output of fresh water per unit area was 18.25 L. It happened due to the fact that the increase in air flow rate enhances mass and heat transfer coefficients inside the humidifier, which further enhances the rate of vaporization of water and, hence, the unit production of fresh water. They have also compared different configurations. Kabeel and El-Said [26–28] have presented the review of fresh water production and strategies for its development.

–From the literature survey, it is found that the development of analytical characteristic equation for double slope solar distiller unit augmented with N identical parabolic concentrator integrated evacuated tubular collector (NPCETCDS) has not been reported so far. So, the analytical characteristic equation for NPCETCDS has been developed which is also applicable for NETCDS reported by Singh and Tiwari [5] and PDS. Recently Mishra et al. [29] have reported the energy metrics analysis of N alike parabolic concentrator

coupled with evacuated tubular collectors (PCETCs) in which N alike PCETCs were arranged in series and they were kept in open loop. However, in the proposed NPCETCDS, N alike PCETCs have been arranged in series and they have been kept in closed loop as outlet of N th PCETC goes into basin and inlet of 1st PCETC takes fluid from basin through pump. The values of instantaneous efficiency for NPCETCDS have been computed using MATLAB and the result has been compared with the result of NETCDS and PDS. The proposed NPCETCDS is different from the desalination system reported by Singh and Tiwari [18] in the sense that parabolic surface has been integrated with ETCs in the case of NPCETCDS.

2. Explanation of NPCETCDS

The schematic diagram of NPCETCDS has been presented in Fig. 1 and its specification is represented by Table 1. The elevated side view of the first PCETC is presented in Fig. 2. If collectors are arranged in parallel, discharge is higher but temperature of fluid at the outlet of collector is low. Contrary to this, if collectors are arranged in series, discharge is low but temperature is high at the outlet of the last collector. In the proposed solar desalination unit, series arrangement has been considered as the prime objective of coupling collector with basin; this is to enhance temperature of water in the basin.

In series arrangement of collectors, the exit of each collector is linked to the entry of its following collectors. Fluid to entrance of 1st collector comes from basin through variable discharge pump. Fluid gains heat from solar intensity while flowing through tubes of collector and fluid which is available at higher temperature at the exit of last collector goes to the basin again. Thus, a closed loop is formed. Collectors are tilted at 30° (approximately equal to latitude of place) with horizontal surface with an objective of receiving highest annual solar energy.

The double slope solar desalination unit in this effort has been made up of glass reinforced plastic with the basin area of 2 m^2 . The orientation of desalination unit is kept toward east-west with an objective of receiving maximum annual solar energy. The condensing cover surface is tilted by 15° with the horizontal surface and the condensing surface is made up of transparent glass. There are two holes – one at the back wall which is used to supply saline/brackish water to basin and the other hole at underside which may be used for cleaning basin when required to do so. A provision of iron stand is made for supporting the whole unit.

When solar radiation impinges on the outer surface of condensing cover, first of all reflection takes place followed by the absorption and transmission. The transmitted radiation falls on the surface of water in the basin. Again, reflection occurs followed by absorption and transmission. Some part of radiation is retained by water mass and the remaining part of radiation goes to the blackened surface at the bottom of basin where almost all radiation coming to the plane gets absorbed. The temperature of basin liner increases which in turn transfers heat to water in basin. In this way, water gets heat from direct solar radiation as well as indirect heat gain through basin liner and a number of collectors. It results in increasing the temperature of water and a temperature

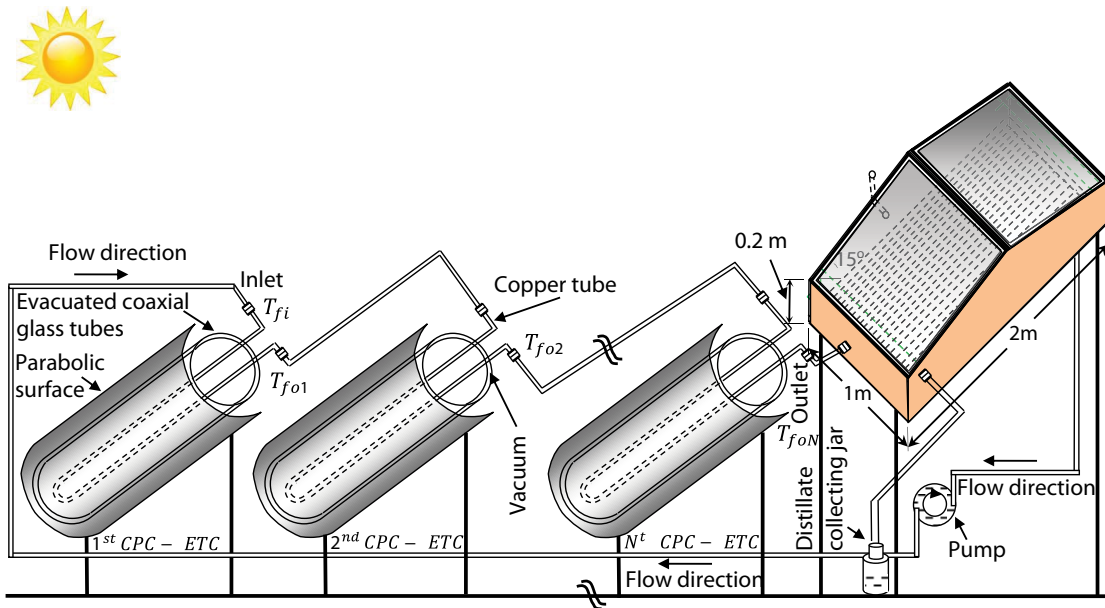


Fig. 1. Schematic diagram of proposed N alike parabolic concentrator collected incorporated with double slope solar still (NPCETCDS).

Table 1
Specifications of double slope solar distiller unit augmented with N identical parabolic concentrator integrated evacuated tubular collectors (NPCETCDS)

Double slope active solar still			
Component	Specification	Component	Specification
Length	2 m	Cover material	Glass
Width	1 m	Orientation	East-west
Inclination of glass cover	15°	Thickness of glass cover	0.004 m
Height of smaller side	0.2 m	K_g	0.816 W/m-K
Material of body	GRP	Thickness of insulation	0.1 m
Material of stand	GI	K_i	0.166 W/m-K
Parabolic concentrator integrated evacuated tubular collectors (PCETC)			
Component	Specification	Component	Specification
Type and no. of collectors	PCETC, N	α_p	0.8
DC motor rating	12 V, 24 W	F'	0.986
Diameter of inner copper tube	0.0125 m	τ_g	0.95
Thickness of copper tube	0.0005 m	K_g (Wm ⁻¹ K ⁻¹)	1.09
Outer radius of outer glass tube of evacuated coaxial glass	0.024 m	Angle of PCETC Horizontal	30°
Inner radius of inner glass tube of evacuated coaxial glass	0.0165 m	Length of each copper Tube	2.0 m
Thickness of outer/inner of evacuated coaxial glass	0.002 m	Reflectivity	0.85
		Aperture area	0.82896 m ²
		Receiver area	0.27632 m ²

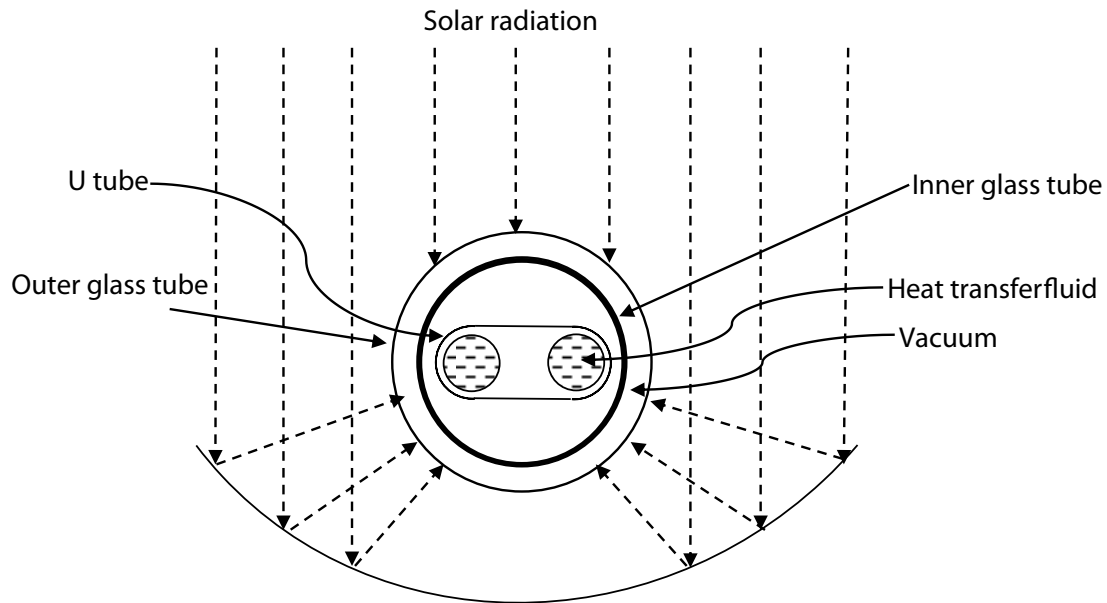


Fig. 2. Elevated view of parabolic concentrator integrated evacuated tubular collector.

difference is created between the surface of water in basin and inner surface of condensing cover. Due to this temperature difference, evaporation of water occurs and vapor in turn gets condensed at the inner surface of condensing cover which trickles down and gets collected in the tray fixed to the inner surface of lower wall. Fresh water from the tray is collected in a jar through pipe.

3. Thermal modeling

The characteristic equation development for NPCETCDS involves the thermal modeling for NPCETCDS. The thermal modeling of the system is carried out by writing equations for different components on the basis of balancing energy. The various equations so obtained are then solved to get the expression of unknown parameters in terms of known parameters. Assumptions for writing energy balance equations for different components of NPCETCDS are as follows:

- The proposed NPCETCDS is in quasi steady state condition.
- The variation in temperature across the thickness of insulating and glass materials is negligible.
- Condensing covers, absorbing and insulating materials have negligible small heat capacity.
- Heat flow has been considered as one dimensional.
- The seepage of vapor through joints in solar distiller unit is negligible.
- The depth of water in solar distiller unit is kept constant.
- The formation of layers in water mass kept in the basin does not take place.
- The condensation having film type characteristic takes place at inside plane of condensing cover.

Equations for different components of NPCETCDS on the ground of equating net energy input to net energy output can be written as follows:

3.1. For N alike parabolic concentrator integrated evacuated tubular collector (PCETC) arranged in series

3.1.1. For receiver/absorber

When solar flux falls on the plane of parabolic concentrator integrated evacuated tubular collector, the beam radiation gets reflected from the surface of concentrator and impinges on the surface lying outside of outer glass tube of coaxial evacuated tubes. Some parts get reflected from the surface lying outside of outer glass tube of coaxial evacuated tubes, some parts get absorbed by outer glass tube and the rest is transmitted to the surface lying outside of inner glass tube. The space between two coaxial glass tubes is evacuated. Again, from the outer surface of inner glass tube, some part of radiation gets reflected, some parts are absorbed and the remaining parts of radiation are transmitted to the blackened surface. The blackened surface which acts as the receiver/absorber plate lies at the inside surface of inner glass tube. This plate transfers heat to fluid that flows inside the tube made up of copper. The heat is also lost to the ambient through two glass surfaces. The temperature of copper tube and fluid flowing through the copper tube has been assumed same. Hence, following Mishra et al. [29], equation for blackened surface (receiver) of 1st PCETC of N alike PCETCs in closed loop on the basis of balancing the energy can be expressed as:

$$\alpha\tau^2\rho I_b A_a = Fh_{pf}(T_p - T_f)A_r + U_{tpa}(T_p - T_a)A_r \quad (1)$$

where

$$U_{tpa} = \left[\frac{R_0 \ln\left(\frac{R_{i2}}{R_{i1}}\right)}{K_g} + \frac{1}{C_{ev}} + \frac{R_{o2} \ln\left(\frac{R_{o2}}{R_{o1}}\right)}{K_g} + \frac{1}{h_o} \right]^{-1} \quad (2)$$

and

$$h_o = 5.7 + 3.8V \tag{3}$$

Here h_{pf} , U_{tpa} and h_o stand for HTC from plate to fluid, overall HTC from plate to environment through two glass surfaces and total HTC from surface of outer glass tube lying outside respectively. The term on left hand side (LHS) of Eq. (1) corresponds to heat per unit time available on the blackened surface. The second term on right hand side (RHS) of Eq. (1) corresponds to the amount of heat transferred from blackened surface to fluid per unit time. 2nd term on RHS of Eq. (1) corresponds to heat lost to the environment through two surfaces of glass. Here $A_r = 2\pi R_{o1}L$ and R_{o1} is the inner radius of outer glass tube.

3.1.2. For fluid passing through copper tubes of PCETC

The fluid flowing through copper tube receives heat from the blackened surface and the fluid carries the heat away with it. Hence, equation based on balancing the incoming heat to outgoing heat for fluid flowing through copper tubes of N alike PCETCs in closed loop can be written as [20]

$$\dot{m}_f C_f \frac{dT_f}{dx} = F'h_{pf}(T_p - T_f)2\pi r dx \tag{4}$$

where r represents the radius of copper tube and dx represents length of element along the length of tube. LHS of Eq. (4) corresponds to the amount of heat per unit time carried away by the fluid flowing through copper tubes. RHS of Eq. (4) corresponds to heat received by fluid from blackened surface. F' corresponds to collector efficiency factor.

From Eq. (1), T_p can be expressed as

$$T_p = \frac{\alpha\tau^2\rho I_b \frac{A_a}{A_r} + F'h_{pf}T_f + U_{tpa}T_a}{F'h_{pf} + U_{tpa}} \tag{5}$$

Subtracting T_f from both sides in Eq. (3) and rearranging, one can get

$$F'h_{pf}(T_p - T_f) = PF_1\alpha\tau^2\rho I_b(t)\frac{A_a}{A_r} - U_L(T_f - T_a) \tag{6}$$

where

$$PF_1 = \frac{F'h_{pf}}{F'h_{pf} + U_{tpa}} \tag{7}$$

and

$$U_L = \frac{F'U_{tpa}h_{pf}}{F'h_{pf} + U_{tpa}} \tag{8}$$

From Eqs. (4) and (6) one can get

$$\dot{m}_f C_f \left(\frac{dT_f}{dx} \right) = 2\pi r \left[PF_1\alpha\tau^2\rho I_b(t)\frac{A_a}{A_r} - U_L(T_f - T_a) \right] \tag{9}$$

On solving differential equation (Eq. (9)) under boundary conditions:

- when $x = 0, T_f = T_{fi}$ and
- when $x = L, T_f = T_{fo1}$;

one can get the expression of temperature at the outlet of first PCETC (T_{fo1}) as:

$$T_{fo1} = \frac{PF_1(\alpha\tau)_{eff}(A_r F_r)}{\dot{m}_f C_f} I_b(t) + \frac{(A_r F_r)U_L}{\dot{m}_f C_f} T_a + K_K T_{fi} \tag{10}$$

where

$$(\alpha\tau)_{eff} = \rho\alpha\tau^2 \left(\frac{A_a}{A_r} \right) \tag{11}$$

$$(A_r F_r) = \frac{\dot{m}_f C_f}{U_L} \left[1 - \exp \left(-\frac{2\pi r L U_L}{\dot{m}_f C_f} \right) \right] \tag{12}$$

and

$$K_K = 1 - \frac{A_r F_r U_L}{\dot{m}_f C_f} \tag{13}$$

Here, one should note that $T_{fi} = T_{w0}$ as inlet of 1st PCETC takes fluid from basin of the proposed solar distiller through pump inserted between basin and inlet of 1st PCETC.

Using Eq. (10), temperatures at the outlet of second PCETC can be written as

$$T_{fo2} = \frac{PF_1(\alpha\tau)_{eff}(A_r F_r)}{\dot{m}_f C_f} I_b(t) + \frac{(A_r F_r)U_L}{\dot{m}_f C_f} T_a + K_K T_{fi2} \tag{14}$$

The output of first PCETC will be input to the second PCETC, that is, $T_{fo1} = T_{fi2}$ and hence temperature at the outlet of second PCETC (T_{fo2}) using Eq. (14) can be expressed as

$$T_{fo2} = \frac{PF_1(\alpha\tau)_{eff}(A_r F_r)}{\dot{m}_f C_f} I_b(t) + \frac{(A_r F_r)U_L}{\dot{m}_f C_f} T_a + K_K T_{fo1} \tag{15}$$

Substituting T_{fo1} from Eq. (10) into Eq. (15) and rearranging, one can obtain

$$T_{fo2} = \frac{PF_1(\alpha\tau)_{eff}(A_r F_r)(1 - K_K^2)}{\dot{m}_f C_f (1 - K_K)} I_b(t) + \frac{(A_r F_r)U_L(1 - K_K^2)}{\dot{m}_f C_f (1 - K_K)} T_a + K_K^2 T_{fi} \tag{16}$$

Using Eq. (10), the expression for temperature at the outlet of third PCETC can be written as

$$T_{fo3} = \frac{PF_1(\alpha\tau)_{eff}(A_r F_r)}{\dot{m}_f C_f} I_b(t) + \frac{(A_r F_r)U_L}{\dot{m}_f C_f} T_a + K_K T_{fi3} \tag{17}$$

Again, output of second PCETC will be input to third PCETC, that is, $T_{fo2} = T_{fi3}$ and hence temperature at the outlet of third PCETC (T_{fo3}) using Eq. (17) can be written as

$$T_{i03} = \frac{PF_1(\alpha\tau)_{\text{eff}}(A_r F_r)}{\dot{m}_f C_f} I_b(t) + \frac{(A_r F_r)U_L}{\dot{m}_f C_f} T_a + K_K T_{i02} \quad (18)$$

Substituting T_{i02} from Eq. (16) into Eq. (18) and rearranging, one can obtain the expression for T_{i03} as

$$T_{i03} = \frac{PF_1(\alpha\tau)_{\text{eff}}(A_r F_r)(1-K_K^3)}{\dot{m}_f C_f (1-K_K)} I_b(t) + \frac{(A_r F_r)U_L (1-K_K^3)}{\dot{m}_f C_f (1-K_K)} T_a + K_K^3 T_{fi} \quad (19)$$

Proceeding in the similar fashion, one can obtain the expression for the temperature at the exit of N th PCETC and it can be expressed as

$$T_{i0N} = \frac{PF_1(\alpha\tau)_{\text{eff}}(A_r F_r)(1-K_K^N)}{\dot{m}_f C_f (1-K_K)} I_b(t) + \frac{(A_r F_r)U_L (1-K_K^N)}{\dot{m}_f C_f (1-K_K)} T_a + K_K^N T_{fi} \quad (20)$$

where N is the number of parabolic concentrator integrated evacuated tubular collector.

The amount of heat gained per unit time from N alike PC-ETCs can be written as

$$\dot{Q}_{UN} = \dot{m}_f C_f (T_{i0N} - T_{fi}) \quad (21)$$

Putting the expression of T_{i0N} from Eq. (20) into Eq. (21) and rearranging, one can get

$$\dot{Q}_{UN} = (PF_1)(\alpha\tau)_{\text{eff}} \frac{(1-K_K^N)}{(1-K_K)} I_b(t) - (A_r F_r)U_L \frac{(1-K_K^N)}{(1-K_K)} (T_{fi} - T_a) \quad (22)$$

3.2. For solar distiller unit

3.2.1. For outer plane of condensing cover oriented towards east

When solar flux falls on the outer plane of condensing cover oriented towards east, some part of the incoming solar flux gets reflected from outer plane of condensing cover oriented towards east, some part gets absorbed by the condensing surface oriented towards east and the remaining part is transmitted to the inside plane of condensing surface oriented towards east. At the same time, heat per unit time is conducted from inside plane to the outside plane of the condensing cover facing east. Hence, equation based on balancing the energy per unit time for outer plane of condensing cover oriented towards east can be expressed as

$$\frac{K_g}{L_g} (T_{giE} - T_{goE}) A_{gE} = h_{1gE} (T_{goE} - T_a) A_{gE} \quad (23)$$

where h_{1gE} is total HTC from outside plane of condensing cover facing east to ambient. The term on LHS of Eq. (23) corresponds to the amount of heat conducted per unit time from inside plane to the outside plane of the condensing cover oriented towards east. This term has been written using

Fourier's law. The term on RHS of Eq. (23) corresponds to the amount of heat per unit time lost to the ambient through convection and radiation. This term is based on Newton's law of cooling.

3.2.2. For inside plane of condensing cover oriented toward east

The inside plane of condensing cover oriented toward east receives heat from solar flux transmitted from outer plane to the inside plane. The inside plane of condensing shroud also collects heat per unit time from top plane of water through convective, radiative and evaporative heat transfer modes. At the same time, heat is lost per unit time from inside plane to the outside of the condensing cover. It also loses heat per unit time through radiation to the inside plane of condensing cover oriented towards west. Hence, equation for inside plane of condensing drape oriented toward east on the basis of balancing energy per unit time can be expressed as

$$\alpha'_g I_{SE}(t) A_{gE} + h_{1wE} (T_w - T_{giE}) \frac{A_b}{2} - h_{EW} (T_{giE} - T_{giW}) A_{gE} = \frac{K_g}{L_g} (T_{giE} - T_{goE}) A_{gE} \quad (24)$$

where h_{1wE} represents total HTC from outermost plane of water mass kept in basin to inside plane of condensing cover oriented towards east, h_{EW} stands for HTC from inside plane of glass cover facing east to the inside plane of glass cover facing west and α'_g stands for the amount of heat absorbed by glass cover.

First term of LHS in Eq. (24) corresponds to heat absorbed per unit time by the condensing cover. The 2nd term on LHS of Eq. (24) corresponds to the amount of heat received by inside plane of condensing cover per unit time from the surface of water through convective, radiative and evaporative heat transfer modes. The third term on LHS of Eq. (24) corresponds to the amount of heat lost from the inside plane of glass cover oriented towards east to the inside plane of glass cover oriented towards west. The term on RHS of Eq. (24) corresponds to the amount of heat lost per unit time through conduction from inside plane of glass cover facing east to the outside plane of the condensing cover.

3.2.3. For outer plane condensing cover oriented towards west

When solar flux falls on the outer plane of condensing cover oriented towards west, some parts of the incoming solar flux gets reflected from outer plane of condensing cover oriented towards west, some parts get absorbed by the condensing surface oriented towards west and the remaining part is transmitted to the inside plane of condensing surface oriented towards west. At the same time, heat per unit time is conducted from inside plane to the outside plane of the condensing cover facing west. Hence, equation based on balancing the energy per unit time for outer plane of condensing cover oriented towards west can be expressed as

$$\frac{K_g}{L_g} (T_{giW} - T_{goW}) A_{gW} = h_{1gW} (T_{goW} - T_a) A_{gW} \quad (25)$$

where h_{1gW} stands for total HTC from outside plane of condensing cover oriented towards west to ambient.

The term on LHS of Eq. (24) corresponds to the amount of heat conducted per unit time from inside plane to the outside plane of the condensing cover oriented towards west. This term has been written using Fourier’s law. The term on RHS of Eq. (24) corresponds to the amount of heat per unit time lost to the ambient through convective and radiative heat transfer modes. This term is based on Newton’s law of cooling.

3.2.4. For inside plane of condensing cover oriented toward west

The inside plane of condensing cover oriented toward west receives heat from solar flux transmitted from outer plane to the inside plane. The inside plane of condensing shroud also gains heat per unit time from top plane of water in basin through convective, radiative and evaporative modes of heat transfer. It also receives heat per unit time through radiative mode of heat transfer from inside plane of condensing cover oriented towards east. At the same time, heat per unit time is lost from inside plane to the outside plane of condensing cover oriented towards west. Hence, equation for inside plane of condensing cover oriented toward west on the basis of balancing energy per unit time can be expressed as

$$\alpha'_g I_{SW}(t) A_{gW} + h_{1wW} (T_w - T_{giW}) \frac{A_b}{2} + h_{EW} (T_{giE} - T_{giW}) A_{gE} = \frac{K_g}{L_g} (T_{giW} - T_{goW}) A_{gW} \tag{26}$$

where h_{1wW} is total HTC from water surface to inside plane of glass cover facing west.

First term of LHS in Eq. (25) corresponds to the heat absorbed per unit time by the condensing cover oriented towards west. The second term on LHS of Eq. (25) corresponds to the amount of heat received by inside plane of condensing cover per unit time from the surface of water through convective, radiative and evaporative modes of heat transfer. The third term on LHS of Eq. (25) corresponds to the amount of heat gained from the inside plane of glass cover facing east to the inside plane of glass cover facing west. The term on RHS of Eq. (25) corresponds to the amount of heat lost per unit time through conduction from inside plane of glass cover facing west to the outside plane of the condensing cover.

3.2.5. For basin liner

The solar radiation reaches the surface of the basin liner after transmission from water mass kept in basin. Here, almost entire radiation flux falling on the surface of basin liner gets absorbed as the basin liner acts as black body. Temperature of basin liner rises and it becomes higher than the temperature of water in basin. Now, basin liner transfers heat to water in basin through convective and radiative heat transfer modes. Heat is also lost by basin liner to the environment through conduction followed by radiation and

convection. Hence, equation for basin liner based on balancing energy can be written as

$$\alpha'_b (I_{SE}(t) + I_{SW}(t)) \frac{A_b}{2} = h_{bw} (T_b - T_w) A_b + h_{ba} (T_b - T_a) A_b \tag{27}$$

where

$$h_{ba} = \left[\frac{L_i}{K_i} + \frac{1}{h_{cb} + h_{rb}} \right]^{-i} \tag{28}$$

and $h_{bw} = 100 \text{ W/m}^2$

Here α'_b , h_{bw} and h_{ba} correspond to the absorptivity of bottom blackened surface of basin, HTC from basin liner to water kept in basin and HTC from basin liner to atmosphere in that order. The term on LHS of Eq. (16) corresponds to total solar flux engrossed by bottom blackened surface of basin. 1st term on RHS of Eq. (16) corresponds to heat transferred per unit time from bottom blackened surface of basin to water kept in basin. 2nd term on RHS of Eq. (16) corresponds to heat lost per unit time by the basin liner to ambient through conductive heat transfer mode followed by convective and radiative heat transfer modes.

3.2.6. For water mass kept in basin

When solar flux strikes the surface of water mass kept in basin after getting transmitted from glass cover, some part of incoming solar flux gets reflected from water, some parts get engrossed by water and the rest impinging solar flux on the surface of water gets transmitted from glass cover facing both east as well as west to basin liner. Water kept in basin also collects heat from basin liner through convective and radiative heat transfer modes. At the same time, heat from water mass is lost per unit time to inside planes of glass covers facing both east as well as west through convective, radiative and evaporative heat transfer modes. Hence, equation for water mass based on balancing energy can be expressed as

$$(M_w C_w) \frac{dT_w}{dt} = (I_{SE}(t) + I_{SW}(t)) \alpha'_w \frac{A_b}{2} + h_{bw} (T_b - T_w) A_b - h_{1wE} (T_w - T_{giE}) \frac{A_b}{2} - h_{1wW} (T_w - T_{giW}) \frac{A_b}{2} + \dot{Q}_{uN} \tag{29}$$

where Q_{uN} stands for the quantity of heat gained per unit time from series connected N alike PCETCs. Its value can be computed from Eq. (20). The term on LHS of Eq. (28) corresponds to amount of heat per unit time stored in water mass in basin. 1st term on RHS of Eq. (28) corresponds to heat absorbed by water from solar flux coming from both east as well as west glass covers. 2nd term on RHS corresponds to heat transferred per unit time to water mass by bottom blackened surface. 3rd term on RHS of Eq. (28) corresponds to heat energy given by water to inside plane of condensing surface facing east and 4th term on RHS of Eq. (28) corresponds to heat lost by water to inside plane of glass cover facing west.

Eq. (13) can be rearranged as

$$\frac{K_g}{L_g} (T_{giE} - T_{goE}) A_{gE} = U_{cE} (T_{giE} - T_a) A_{gE} \tag{30}$$

where

$$U_{cE} = \frac{\frac{K_g}{L_g} h_{1gE}}{\frac{K_g}{L_g} + h_{1gE}} \quad (31)$$

Using Eqs. (23) and (29), one can get

$$\alpha'_g I_{SE}(t) A_{gE} + h_{1wE} (T_w - T_{giE}) \frac{A_b}{2} - h_{EW} (T_{giE} - T_{giW}) A_{gE} = U_{cE} (T_{giE} - T_a) A_{gE} \quad (32)$$

Similarly, using Eqs. (24) and (25), one can get

$$\alpha'_g I_{SW}(t) A_{gW} + h_{1wW} (T_w - T_{giW}) \frac{A_b}{2} + h_{EW} (T_{giE} - T_{giW}) A_{gW} = U_{cW} (T_{giW} - T_a) A_{gW} \quad (33)$$

where

$$U_{cW} = \frac{\frac{K_g}{L_g} h_{1gW}}{\frac{K_g}{L_g} + h_{1gW}} \quad (34)$$

From Eq. (32) one can get T_{giW} as

$$T_{giW} = \frac{\alpha'_g I_{SW} A_{gW} + h_{1wW} T_w \frac{A_b}{2} + h_{EW} T_{giE} A_{gW} + U_{cW} T_a A_{gW}}{h_{1wW} \frac{A_b}{2} + h_{EW} A_{gW} + U_{cW} A_{gW}} \quad (35)$$

Multiplying both sides by (-1) and adding T_{giE} on both sides and rearranging, one can get

$$T_{giE} - T_{giW} = \frac{h_{1wW} \frac{A_b}{2} (T_{giE} - T_w) + U_{cW} A_{gW} (T_{giE} - T_a) - \alpha'_g I_{SW} A_{gW}}{h_{1wW} \frac{A_b}{2} + h_{EW} A_{gW} + U_{cW} A_{gW}} \quad (36)$$

Substituting $(T_{giE} - T_{giW})$ in Eq. (31) and rearranging, one can get

$$T_{giE} = \frac{(\alpha'_g I_{SE} + U_{cE} T_a) A_{gE} + (\alpha'_g I_{SW} + U_{cW} T_a) \frac{h_{EW}}{U_2} A_{gW} + T_w \left(h_{1wE} \frac{A_b}{2} + \frac{h_{EW}}{U_2} h_{1wW} \frac{A_b}{2} \right)}{h_{1wE} \frac{A_b}{2} + \frac{h_{EW}}{U_2} h_{1wW} \frac{A_b}{2} + U_{cW} A_{gW} \frac{h_{EW}}{U_2} + U_{cE} A_{gE}} \quad (37)$$

where

$$U_2 = h_{1wW} \frac{A_b}{2} + h_{EW} A_{gW} + U_{cW} A_{gW} \quad (38)$$

Eq. (36) can further be rearranged as

$$T_{giE} = \frac{R_1 U_2 A_{gE} + R_2 h_{EW} A_{gW} + T_w \left(h_{1wE} \frac{A_b}{2} + \frac{h_{EW}}{U_2} h_{1wW} \frac{A_b}{2} \right)}{U_2 \left(h_{1wE} \frac{A_b}{2} + h_{EW} A_{gE} + U_{cE} A_{gE} \right) - \frac{h_{EW}^2 A_{gW}}{A_{gE}}} \quad (39)$$

where

$$R_1 = \alpha'_g I_{SE} + U_{cE} T_a \quad (40)$$

$$R_2 = \alpha'_g I_{SW} + U_{cW} T_a \quad (41)$$

After simplifying Eq. (38), one can obtain the expression for T_{giE} as

$$T_{giE} = \frac{A_1 + A_2 T_w}{P} \quad (42)$$

$$A_1 = R_1 U_2 A_{gE} + R_2 h_{EW} A_{gW} \quad (43)$$

$$A_2 = h_{1wE} \frac{A_b}{2} + \frac{h_{EW}}{U_2} h_{1wW} \frac{A_b}{2} \quad (44)$$

$$U_1 = h_{1wE} \frac{A_b}{2} + h_{EW} A_{gE} + U_{cE} A_{gE} \quad (45)$$

$$P = U_2 U_1 - \frac{h_{EW}^2 A_{gW}}{A_{gE}} \quad (46)$$

Substituting T_{giE} from Eq. (41) in Eq. (34) and rearranging one can obtain the expression of T_{giW} as

$$T_{giW} = \frac{(\alpha'_g I_{SW} + U_{cW} T_a) A_{gW} + \left(h_{1wW} \frac{A_b}{2} + \frac{h_{EW} A_{gW} A_2}{P} \right) T_w + \frac{h_{EW} A_{gW} A_1}{P}}{U_2 A_{gE}} \quad (47)$$

Eq. (46) can further be rearranged as

$$T_{giW} = \frac{(R_2 P + h_{EW} A_1) A_{gW} + \left(P h_{1wW} \frac{A_b}{2} + h_{EW} A_{gW} A_2 \right) T_w}{U_2 P A_{gE}} \quad (48)$$

Again rearranging Eq. (47), T_{giW} can be expressed as

$$T_{giW} = \frac{B_1 + B_2 T_w}{P} \quad (49)$$

$$B_1 = \frac{(R_2 P + h_{EW} A_1) A_{gW}}{U_2 A_{gE}} \quad (50)$$

$$B_2 = \frac{P h_{1wW} \frac{A_b}{2} + h_{EW} A_{gW} A_2}{U_2 A_{gE}} \quad (51)$$

Eq. (26) can be expressed as

$$2h_{bw}(T_b - T_w) \frac{A_b}{2} = \alpha'_b h_1 A_b (I_{SE}(t) + I_{SW}(t)) - U_b A_b (T_w - T_a) \quad (52)$$

where

$$h_1 = \frac{h_{bw}}{2(h_{bw} + h_{ba})} \quad (53)$$

and

$$U_b = \frac{h_{ba} h_{bw}}{h_{ba} + h_{bw}} \quad (54)$$

Putting values of T_{giE} from Eq. (41), T_{giW} from Eq. (48) and $(T_b - T_w)$ from Eq. (51) into Eq. (28) and rearranging, one can get

$$M_w C_w \frac{dT_w}{dt} + \left[\begin{aligned} & (A_r F_r) U_L \frac{(1 - K_k^N)}{(1 - K_k)} + U_b A_b + (h_{1wE} + h_{1wE}) \frac{A_b}{2} - \\ & \left(\frac{h_{1wE} A_2}{P} \right) \frac{A_b}{2} - \left(\frac{h_{1wW} B_2}{P} \right) \frac{A_b}{2} \end{aligned} \right] T_w = \left[\begin{aligned} & \left(\frac{\alpha'_w}{2} + h_1 \alpha'_b \right) A_b (I_{SE}(t) + I_{SW}(t)) + U_b A_b T_a + \\ & \frac{(h_{1wE} A_1 + h_{1wW} B_1) A_b}{P} + (PF_1)(\alpha\tau)_{eff} \frac{(1 - K_k^N)}{(1 - K_k)} I_b + \\ & (A_r F_r) U_L \frac{(1 - K_k^N)}{(1 - K_k)} T_a \end{aligned} \right] \quad (55)$$

Eq. (55) can further be rearranged as T

$$\frac{dT_w}{dt} + aT_w = f(t) \quad (56)$$

where

$$a = \frac{1}{M_w C_w} \left[\begin{aligned} & (A_r F_r) U_L \frac{(1 - K_k^N)}{(1 - K_k)} + U_b A_b + (h_{1wE} + h_{1wE}) \frac{A_b}{2} - \\ & \left(\frac{h_{1wE} A_2}{P} \right) \frac{A_b}{2} - \left(\frac{h_{1wW} B_2}{P} \right) \frac{A_b}{2} \end{aligned} \right] \quad (57)$$

$$f(t) = \frac{1}{M_w C_w} \left[\begin{aligned} & \left(\frac{\alpha'_w}{2} + h_1 \alpha'_b \right) A_b (I_{SE}(t) + I_{SW}(t)) + U_b A_b T_a + \\ & \frac{(h_{1wE} A_1 + h_{1wW} B_1) A_b}{P} + (PF_1)(\alpha\tau)_{eff} \frac{(1 - K_k^N)}{(1 - K_k)} I_b + \\ & (A_r F_r) U_L \frac{(1 - K_k^N)}{(1 - K_k)} T_a \end{aligned} \right] \quad (58)$$

Multiplying both sides of Eq. (56) by e^{at} and integrating under the assumptions given in the study by Singh and

Tiwari [30] and taking initial boundary condition as $T_w = T_{w0}$ at $t = 0$, one can obtain the expression for T_w as

$$T_w = \frac{\bar{f}(t)}{a} (1 - e^{-at}) + T_{w0} e^{-at} \quad (59)$$

Here $\bar{f}(t)$ represents the average value of $f(t)$ between time interval 0 and t .

The rate of evaporative heat transfer can be written as

$$\dot{q}_{ew} = \left[h_{ewE} (T_w - T_{giE}) + h_{ewW} (T_w - T_{giW}) \right] \left(\frac{A_b}{2} \right) \quad (60)$$

where

$$h_{ewE} = 16.273 \times 10^{-3} h_{cWE} \left[\frac{P_w - P_{giE}}{T_w - T_{giE}} \right] \quad (\text{Cooper [31]}) \quad (61)$$

$$h_{ewW} = 16.273 \times 10^{-3} h_{cWW} \left[\frac{P_w - P_{giW}}{T_w - T_{giW}} \right] \quad (\text{Cooper [31]}) \quad (62)$$

$$h_{cWE} = 0.884 \left[(T_w - T_{giE}) + \frac{(P_w - P_{giE})(T_w + 273)}{268.9 \times 10^3 - P_w} \right]^{\frac{1}{3}} \quad (\text{Dunkle [32]}) \quad (63)$$

$$h_{cWW} = 0.884 \left[(T_w - T_{giW}) + \frac{(P_w - P_{giW})(T_w + 273)}{268.9 \times 10^3 - P_w} \right]^{\frac{1}{3}} \quad (\text{Dunkle [32]}) \quad (64)$$

$$P_w = \exp \left[25.317 - \frac{5144}{T_w + 273} \right] \quad (65)$$

$$P_{giE} = \exp \left[25.317 - \frac{5144}{T_{giE} + 273} \right] \quad (66)$$

$$P_{giW} = \exp \left[25.317 - \frac{5144}{T_{giW} + 273} \right] \quad (67)$$

The hourly production of fresh water can be evaluated as

$$\dot{m}_{ew} = \frac{\dot{q}_{ew}}{L'} \times 3600 \quad (68)$$

The instantaneous thermal efficiency (η_i) for NPCETCDS can be written as

$$\eta_i = \frac{\dot{q}_{ew}}{NA_a I_b(t) + A_{gE} I_{SE}(t) + A_{gW} I_{SW}(t)} = \frac{(h_{ewE} (T_w - T_{giE}) + h_{ewW} (T_w - T_{giW})) \left(\frac{A_b}{2} \right)}{NA_a I_b(t) + A_{gE} I_{SE}(t) + A_{gW} I_{SW}(t)} \quad (69)$$

Substituting the value of T_{giE} from Eq. (41), T_{giW} from Eq. (48) and T_w from Eq. (58) in Eq. (33), one can get

$$\eta_i = \left(\frac{A_b}{2P} \right) \left[\frac{\left\{ h_{ewE} (P - A_2) + h_{ewW} (P - B_2) \right\} \left[\frac{\bar{f}(t)}{a} (1 - e^{-at}) + T_{w0} e^{-at} \right] - \{ h_{ewE} A_1 + h_{ewW} B_1 \}}{[NA_{am} I_b(t) + A_{gE} I_{SE}(t) + A_{gW} I_{SW}(t)]} \right] \quad (70)$$

Putting values of P from Eq. (45), A_1 from Eq. (42), A_2 from Eq. (43), B_1 from Eq. (49) and B_2 from Eq. (50) in Eq. (69) and rearranging, one can get

$$\eta_i = \left(\frac{A_b}{H} \right) \left[\frac{1}{\{NA_{am} I_b(t) + A_{gE} I_{SE}(t) + A_{gW} I_{SW}(t)\}} \right] \left[\frac{\left\{ h_{ewE} (E_1 + E_2) + h_{ewW} (E'_1 + E'_2) \right\}}{H'_{11} + H'_{22}} \right] \left[\frac{\left\{ (K_{1E} + \alpha_{wb}) I_{SE}(t) + (K_{1W} + \alpha_{wb}) I_{SW}(t) + \left(\frac{2H}{A_b} \right) \left(\frac{1 - K_K^N}{1 - K_K} \right) (PF)_1(\alpha t)_{eff} I_b(t) \right\} (1 - e^{-at})}{\left\{ K'_{1E} I_{SE}(t) + K'_{1W} I_{SW}(t) \right\} e^{at} + T_{w0} - T_a (H'_{11} + H'_{22}) e^{-at}} \right] \quad (71)$$

Expressions for various unknown terms used in Eq. (71) are given in Appendix-A.

Eq. (71) can further be rearranged as

$$\eta_i = F'_{1g} \left[\frac{X_{11} Y_{11} - \{K'_{1E} I_{SE}(t) + K'_{1W} I_{SW}(t)\} e^{at}}{\{NA_{am} I_b(t) + A_{gE} I_{SE}(t) + A_{gW} I_{SW}(t)\} + (H'_{11} + H'_{22})} + \frac{(T_{w0} - T_a)}{\{NA_{am} I_b(t) + A_{gE} I_{SE}(t) + A_{gW} I_{SW}(t)\}} \right] \quad (72)$$

Expressions for various unknown terms used in Eq. (73) are given in appendix-A.

In Eq. (72)

- If $A_a = A_j$; $\rho = 1$ and $I_b(t) = I(t)$, then characteristic equation for N alike ETCs integrated with double slope solar distillation system will be obtained.
- If $N = 0$, then characteristic equation for double slope passive solar distillation system will be obtained

Values of hourly thermal exergy for NPCETCDS, NETCDS and double slope passive solar distiller unit can be computed as follows:

$$\dot{E}x = \left[h_{ewE} \frac{A_b}{2} [(T_w - T_{giE}) - (T_a + 273) \ln \left\{ \frac{T_w + 273}{T_{giE} + 273} \right\}] + \left[h_{ewW} \frac{A_b}{2} [(T_w - T_{giW}) - (T_a + 273) \ln \left\{ \frac{T_w + 273}{T_{giW} + 273} \right\}] \right] \quad (73)$$

Values of h_{ewE} , h_{ewW} , T_w , T_{giE} and T_{giW} can be computed using Eqs. (61), (62), (59), (42) and (49), respectively. Then, the value of hourly exergy for NPCETCDS can be computed with the help of Eq. (73). The value of daily exergy for the proposed system can be computed by adding hourly exergy output for 24 h. Similarly, value of daily exergy for NETCDS can be computed.

4. Methodology

The computation of yield and instantaneous efficiency for NPCETCDS using the computational program written in MATLAB can be expressed as follows:

Step I

The data of solar intensity on plane in horizontal position and atmospheric temperature have been taken from IMD Pune, India. The expression given by Liu and Jordan formula [33] has been used to evaluate value of intensity on the inclined surface. It was done by writing programming codes in MATLAB.

Step II

Values of T_{foN} , T_w , T_{giE} and T_{giW} have been evaluated with the help of Eqs. (19), (58), (41) and (46), respectively.

Step III

Values of different HTC's have been evaluated from Eqs. (60)-(63) and expressions presented in appendix-A followed by computation of amount of hourly production of fresh water using Eq. (67).

Step IV

The value of instantaneous efficiency has been computed using Eq. (71) and then characteristic curves shown in Fig. 6 have been drawn.

Step V

The values of hourly exergy output for NPCETCDS, NETCDS double slope passive solar distiller unit has been computed using Eq. (72).

For better understanding of methodology, flow chart about methodology for the computation of instantaneous efficiency and exergy has been drawn as follows:

5. Results and discussion

The value of instantaneous efficiency can be computed for an archetypal day in May. Values of global radiation on the horizontal surface, direct radiation on the horizontal surface and atmospheric temperature have been taken from Indian Meteorological Department, Pune, India and their variations are presented by Fig. 3. Mean velocity of air for May is 4.02 m/s. Global radiation and direct radiation for the plane tilted at 30° north latitude has been computed considering the expression reported by Liu and Jordan formula [33]. A computational program in MATLAB has been used for the same. The computation of instantaneous efficiency has been done for eight PCETCs, flow of fluid mass per unit time (\dot{m}_f) = 0.012 kg/s and water depth = 0.14 m.

The variation of various temperatures has been shown in Fig. 4. From this figure, it is seen that the value of T_{foN} is higher than the value of T_w because water from the outlet of

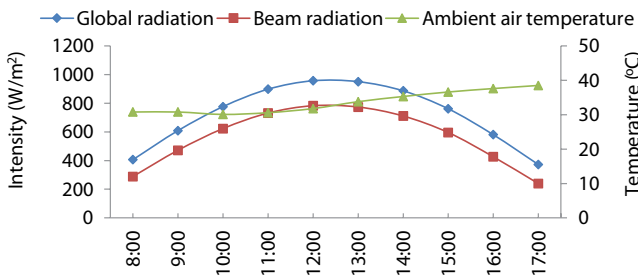
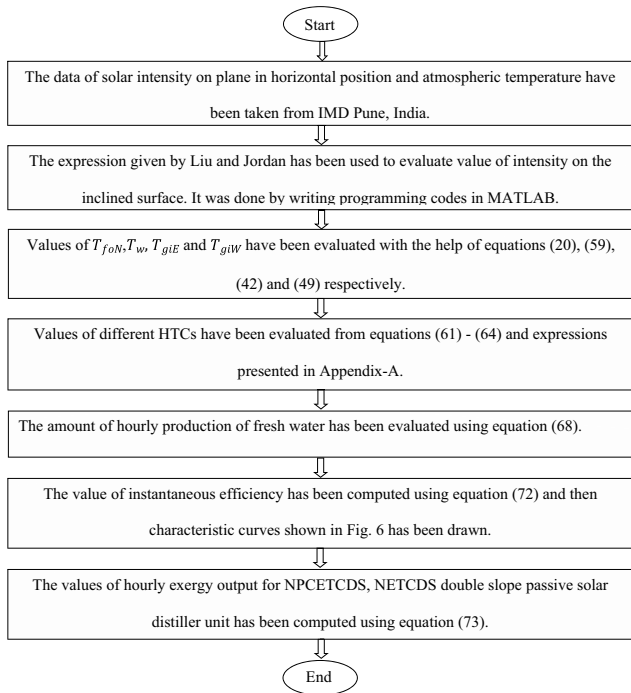


Fig. 3. Hourly solar flux on the surface in horizontal position and surrounding atmospheric temperature for an archetypal day of May.

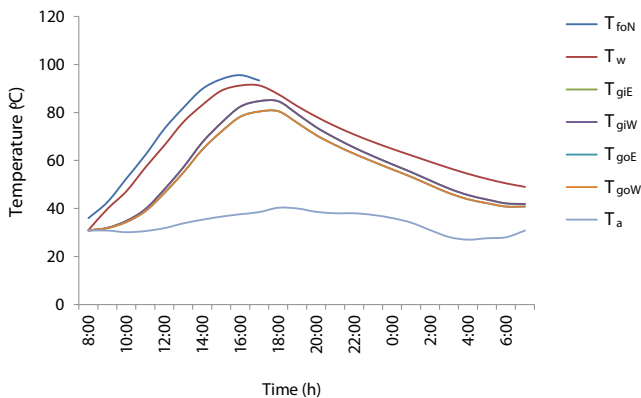


Fig. 4. Variation of different temperatures for NPCETCDS for an archetypal day of May (N = 8).

Nth collectors flows to the basin where it get mixed with the water kept in basin which is at comparatively lower temperature. Further, the temperature of condensing cover made up of glass is less than the temperature of water mass in basin

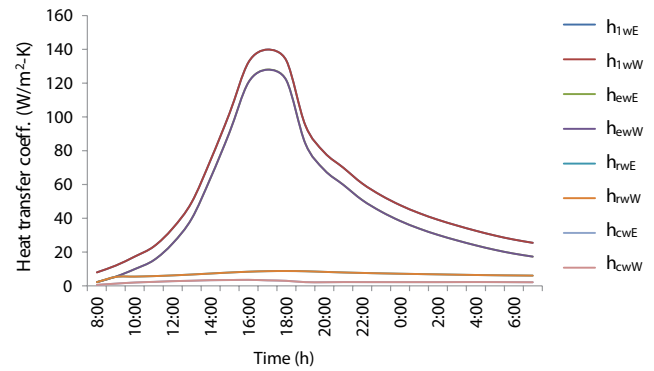


Fig. 5. Variation of different HTCs of NPCETCDS for an archetypal day of May (N = 8).

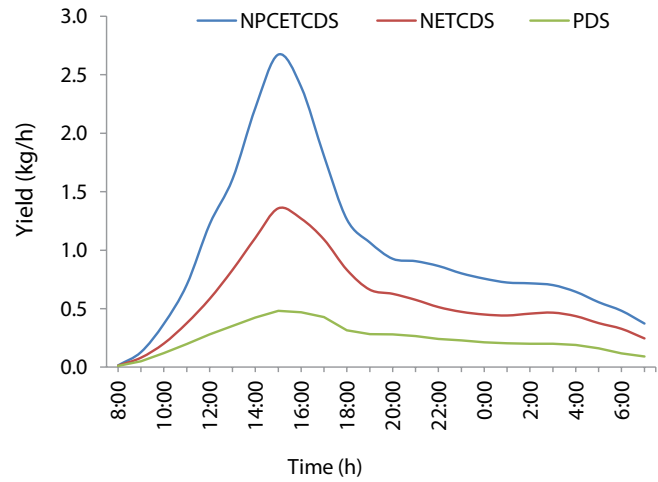


Fig. 6. Hourly generation of fresh water from NPCETCDS for an archetypal day of May (N = 8).

because condensing cover remains in touch with atmospheric and heat energy is being lost to surrounding atmospheric through convective and radiative heat transfer modes. A temperature difference is created between water surface and inner surface of glass cover and this temperature difference is responsible for evaporation of water. This evaporated water is converted into fresh water by rejecting its latent heat at the inside plane of glass cover and moves down under gravity to the channel fixed at the lower side of solar distiller.

Fig. 5 represents the variation of different HTCs for NPCETCDS for a typical day in the month of May. It is observed from Fig. 5 that the value of evaporative HTC is highest between 5 pm and 6 pm. It happens because evaporative HTC is inversely proportional to the difference in values of T_w and T_{gi} and the difference of values of T_w and T_{gi} is minimum at that time. Further, radiative and convective HTCs are very small and they are responsible for losses as they do not contribute to the generation of fresh water. The evaporative HTC is responsible for the generation of fresh water.

Fig. 6 represents variation of hourly generation of fresh water for NPCETCDS, NETCDS and PDS for an archetypal day in May month. Values of mass flow rate and N have been taken as 0.012 kg/s and 8, respectively. It is observed from

Fig. 6 that the production of fresh water from NPCETCDS is highest followed NETCDS and PDS for the same basin area, same values of N , water depth and \dot{m}_f . The generation of fresh water from NPCETCDS is higher than the corresponding values for NETCDS because the rate of heat addition by NPCETCs is higher than the rate of heat addition by NETCs for the same value of N , \dot{m}_f , depth of water and basin area. It further happens because of the integration of parabolic surface in the case of NPCETCs. The generation of fresh water from PDS is lowest because no collector is present in this case which results in comparatively low increase in water temperature. Due to the absence of collector in PDS, the difference in temperatures of water and inside plane of glass cover is comparatively lowest and hence lowest output. Also, the yield is maximum at 3 pm for all three systems because it is related to the multiplication of evaporative HTC and difference in temperature of water surface and inner surface of condensing cover. Similarly, value of thermal exergy for NPCETCDS is highest followed by NETCDS and PDS as shown in Fig. 7.

Fig. 8 represents the variation of daily yield as well as daily exergy for NPCETCDS, PETCDS and PDS for same basin area, same values of water depth, N and \dot{m}_f . The generation of fresh water as well as thermal exergy has been found

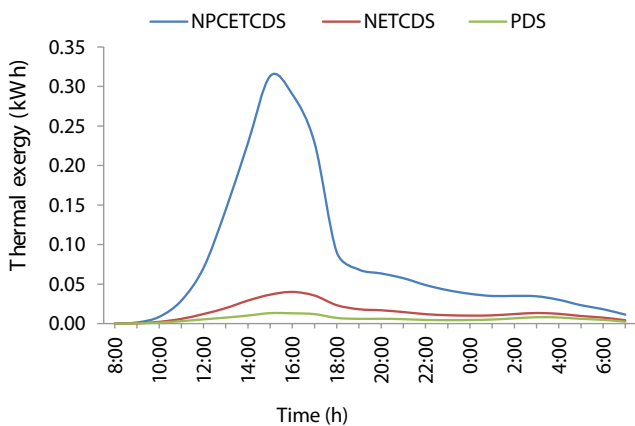


Fig. 7. Variation of hourly thermal exergy of N-PC-ETC-DS and NETCDS for an archetypal day in the month of May ($N = 8$).

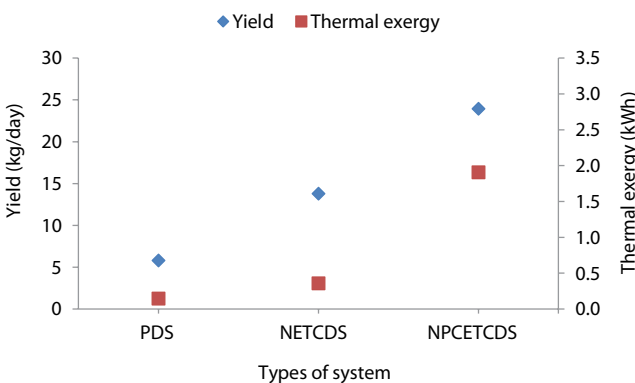


Fig. 8. Variation of daily yield and daily thermal exergy of NPCETCDS, NETCDS and PDS for a typical day in the month of May ($N = 8$).

to be highest for NPCETCDS followed by NETCDS and PDS. The value of daily generation of fresh water is higher by 42.32% and 75.76% for NPCETCDS than NETCDS and PDS in that order. It happens because the amount of heat addition by NPCETCs is higher in the case of NPCETCDS because of the presence of parabolic surface in the case of NPCETCDS; whereas, no collector is present in the case of PDS. The value of daily exergy for NPCETCDS has been found to be higher by 81.17% and 92.25% than NETCDS and PDS, respectively, at the same number of collectors, same water depth and same amount of mass flowing per unit time. It happened due to similar variation in hourly thermal exergy as daily thermal exergy is the addition of hourly thermal exergy for 24 h.

Fig. 9 represents the characteristic curves for NPCETCDS, NETCDS and PDS for an archetypal day of May month. The average value of efficiency for NPCETCDS is higher by 46.18% and 56.99%, respectively. The value of instantaneous efficiency of NPCETCDS is higher than the corresponding value for NETCDS because the amount of heat added by NPCETCs to the basin is higher than the amount of heat added by NETCs. It has been found to occur due to the presence of parabolic surface in the case of NPCETCs which reflects the beam radiation to the receiver area and hence higher amount of heat addition to basin in the case of NPCETCDS as compared with NETCDS. In the case of PDS, no collectors are present and hence value of instantaneous efficiency is lowest due to the similar variation in the generation of fresh water. It is also observed that values of instantaneous efficiency are highest in the evening for all the three systems because input becomes very low whereas output continues to be generated at reasonable rate because of the presence of sensible heat in water mass.

Fig. 10 represents effect of reflectivity on hourly variation of instantaneous efficiency for NPCETCDS for an archetypal day of May at selected number of PCETCs and amount of heat flow per unit time and keeping concentration ratio constant. It is observed from Fig. 10 that the value of instantaneous efficiency increases as the reflectivity is increased. It happens because larger portion of beam radiation will be directed to the surface of receiver and hence greater amount of heat energy per unit time is added to the basin. Fig. 11

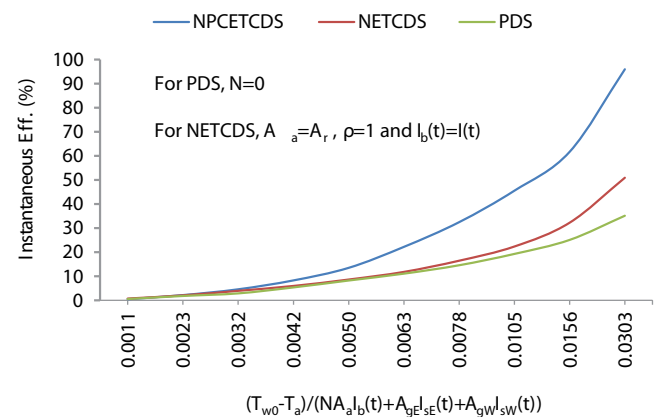


Fig. 9. Hourly variation of instantaneous efficiency of NPCETCDS, NETCDS and PDS for a typical day in the month of May ($N = 8$).

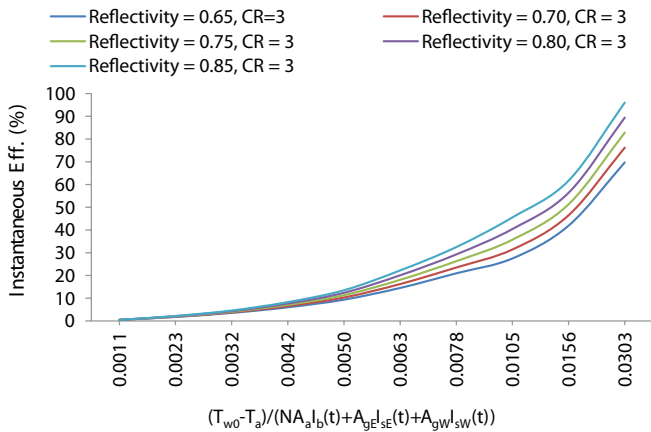


Fig. 10. Effect of reflectivity on hourly variation of instantaneous efficiency of NPCETCDS for a typical day in the month of May ($N = 8$).

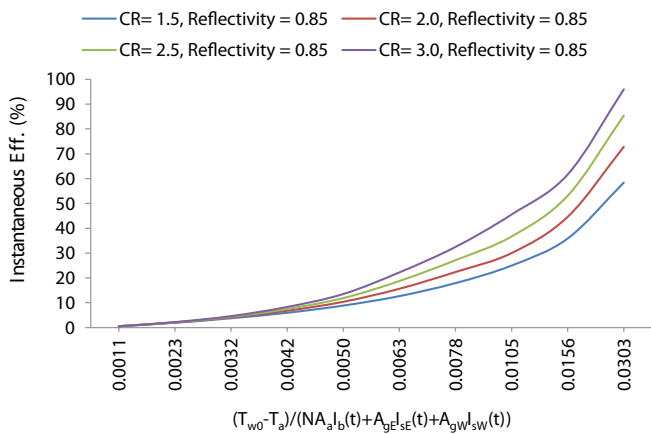


Fig. 11. Effect of concentration ratio on hourly variation of instantaneous efficiency for NPCETCDS for a typical day in the month of May ($N = 8$).

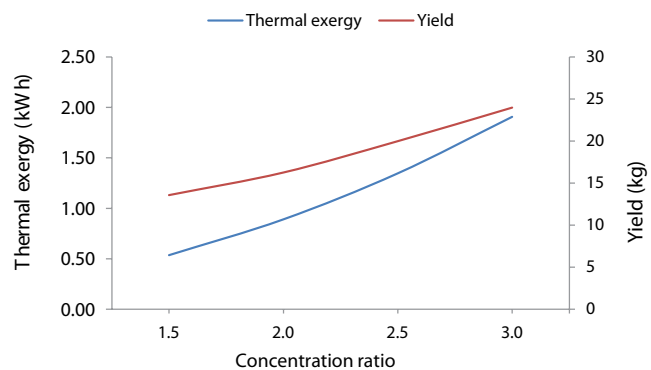


Fig. 12. Effect of concentration ratio on daily thermal exergy and daily yield for NPCETCDS for a typical day in the month of May ($N = 8$).

represents effect of concentration ratio on hourly variation of instantaneous efficiency for NPCETCDS for an archetypal day of May at selected number of PCETCs, amount of mass flow per unit time and keeping reflectivity constant.

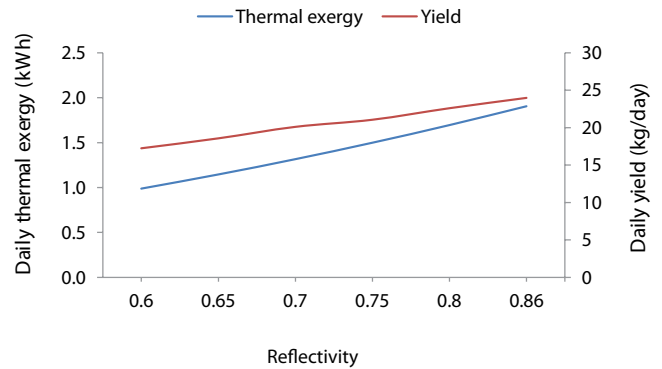


Fig. 13. Effect of reflectivity on daily thermal exergy and daily yield for NPCETCDS for a typical day in the month of May ($N = 8$).

It is observed from Fig. 11 that the value of instantaneous efficiency increases with the increase in concentration ratio. It happens because increased value of concentration ratio results in increased solar beam flux to be directed on the receiver surface. So, higher amount of heat is added to basin which results in increase in values in instantaneous efficiency.

Fig. 12 represents the effect of variation of concentration ratio on daily exergy output and daily generation of fresh water for NPCTCDS for an archetypal day of May at selected number of collectors and the amount of mass flowing per unit time. It has been observed from Fig. 12 that the values of daily exergy and daily generation of fresh water for NPCETCDS increase with the increase in the value of concentration ratio at given value of reflectivity of concentrating surface. It happens because increase in the value of concentration ratio at given value of reflectivity means addition of more heat to basin as larger solar beam flux will be directed to receiver surface. Fig. 13 represents the effect of reflectivity on daily thermal exergy and daily yield for NPCETCDS for an archetypal day of May at given concentration ratio, selected number of NPCETCs and amount of fluid flowing through the copper tube per unit time. Increase in reflectivity means higher radiation is directed to the receiver surface and hence higher heat addition to basin which results in increase in values of thermal exergy as well as yield.

6. Conclusions

The analysis has been done for NPCETCDS and results of the proposed system have been compared with results of NETCDS and PDS. From the present research study, the following conclusions have been drawn:

- The characteristic equation for NPCETCDS has been developed considering the energy balance equation for the proposed system which is similar to Hottel-Whillier-Bliss equation for the flat plate collector. The developed equation is also valid for NPCETCDS and PDS.
- The average value of instantaneous efficiency for NPCETCDS is higher by 46.18% and 56.99% than NETCDS and PDS in that order.
- The value of daily generation of fresh water is higher by 42.32% and 75.76%; the daily thermal exergy is higher by 81.17% and 92.25% for NPCETCDS than NETCDS and

PDS, respectively, at selected number of collectors and amount of mass flowing per second.

- Values of instantaneous efficiency, hourly generation of fresh water and hourly exergy output for the proposed NPCETCDS have been found to increase with the increase in the value of concentration ratio for given reflectivity of concentrating surface.
- Values of instantaneous efficiency, hourly generation of fresh water and hourly exergy output for the proposed NPCETCDS have been found to increase with the increase in the value of reflectivity for the given concentration ratio.

Recommendation

The development of characteristic equation for NPCETCDS has been done and values of instantaneous efficiency and hourly yield have been computed. However, the experimental validation has not been done. So, experimental validation of the proposed system should be done before installing on commercial scale.

Symbols

A_b	— Area of basin, m ²
A_{g^E}	— Area of east glass cover, m ²
A_{g^W}	— Area of west glass cover, m ²
C	— Specific heat capacity, J/kg-K
DS	— Double slope solar still
ETC	— Evacuated tubular collector
F'	— Collector efficiency factor, dimensionless
h_{cw}	— Convective heat transfer coefficient from water to inner surface of glass cover, W/m ² K
h_{ewE}	— Evaporative heat transfer coefficient from water surface to inner surface of east glass cover, W/m ² K
h_{ewW}	— Evaporative heat transfer coefficient from water surface to inner surface of west glass cover, W/m ² K
h_c	— Convective heat transfer coefficient, W/m ² K
h_{ba}	— Heat transfer coefficient from blackened surface to ambient, W/m ² K
h_{bw}	— Heat transfer coefficient from blackened surface to water mass, W/m ² K
h	— Heat transfer coefficient, W/m ² K
h_{rw}	— Radiative heat transfer coefficient from water to inner surface of glass cover, W/m ² K
h_r	— Radiative heat transfer coefficient, W/m ² K
h_{1w}	— Total heat transfer coefficient from water surface to inner glass cover, W/m ² K
h_{1g}	— Total heat transfer coefficient from outer surface of glass to the environment, W/m ² K
h_{EW}	— Radiative heat transfer coefficient from inner surface of east glass cover to inner surface of west glass cover
$I(t)$	— Total solar flux, W/m ²
$I_b(t)$	— Beam radiation on collector, W/m ²
$I_{SE}(t)$	— Solar intensity on east glass cover, W/m ²

$I_{SE}(t)$	— Solar intensity on west glass cover, W/m ²
K	— Thermal conductivity, W/m-K
L_g	— Thickness of glass cover, m
L^{\ddagger}	— Latent heat, J/kg
L	— Length, m
\dot{m}_f	— Mass flow rate of fluid/water, kg/s
\dot{m}_{ew}	— Mass of distillate from double slope solar still, kg
N	— Number of parabolic concentrator integrated evacuated tubular collector
NPCETCDS	— Double slope solar distiller unit augmented with N identical parabolic concentrator integrated evacuated tubular collectors
NETCDS	— Double slope solar still coupled with N alike ETCs
PCETC	— Parabolic concentrator integrated evacuated tubular collectors
PF_1	— Penalty factor first, dimensionless
Q_{UN}	— Useful energy gain for N identical collector connected in series, kWh
R_{o1}	— Inner radius of outer glass tube of evacuated coaxial glass tube, m
R_{i1}	— Inner radius of inner glass tube of evacuated coaxial glass tube, m
R_{i2}	— Outer radius of inner glass tube of evacuated coaxial glass tube, m
R_{o2}	— Outer radius of outer glass tube of evacuated coaxial glass tube, m
CR	— Concentration ratio
r	— Radius of copper tube in ETC
ρ	— Reflectivity
T_{foN}	— Outlet water temperature at the exit of Nth PCETC, °C
T_a	— Ambient temperature, °C
T_{g^E}	— Temperature at inside plane of condensing cover oriented towards east, °C
T_{g^W}	— Temperature at inside plane of condensing cover oriented towards west, °C
T	— Time, h
T_{wo}	— Water temperature at $t = 0$, °C
T_w	— Water temperature, °C
U_L	— Overall heat transfer coefficient
V	— Velocity of air, m/s

Subscript

b	— Basin liner
P	— Pltae
E	— East
eff	— Effective
f	— Fluid
g	— Glass
in	— Incoming
out	— Outgoing
w	— Water
W	— West

Greek letters

α	— Absorptivity (fraction)
η	— Efficiency, %

$(\alpha\tau)_{\text{eff}}$	– Product of effective absorptivity and transmittivity
σ	– Stefan–Boltzmann constant, $\text{W/m}^2 \text{K}^4$
τ	– Transmissivity

References

- [1] S.N. Rai, G.N. Tiwari, Single basin solar still coupled with flat plate collector, *Energy Convers. Manage.*, 23 (1983) 145–149.
- [2] R. Dev, G.N. Tiwari, Characteristic equation of a passive solar still, *Desalination*, 245 (2009) 246–265.
- [3] R. Dev, H.N. Singh, G.N. Tiwari, Characteristic equation of double slope passive solar still, *Desalination*, 267 (2011) 261–266.
- [4] D.B. Singh, V.K. Dwivedi, G.N. Tiwari, N. Kumar, Analytical characteristic equation of N identical evacuated tubular collectors integrated single slope solar still, *Desal. Wat. Treat.*, 88 (2017) 41–51.
- [5] D.B. Singh, G.N. Tiwari, Analytical characteristic equation of N identical evacuated tubular collectors integrated double slope solar still, *J. Solar Energy Eng., ASME*, 135 (2017) 051003.
- [6] V.S. Gupta, D.B. Singh, R.K. Mishra, S.K. Sharma, G.N. Tiwari, Development of characteristic equations for PVT-CPC active solar distillation system, *Desalination*, 445 (2018) 266–279.
- [7] R. Dev, G.N. Tiwari, Annual performance of evacuated tubular collector integrated solar still, *Desal. Wat. Treat.*, 41 (2012) 204–223.
- [8] R. Sathyamurthy, S.A. El-Agouz, P.K. Nagarajan, J. Subramani, T. Arunkumar, D. Mageshbabu, B. Madhu, R. Bharathwaaj, N. Prakash, A Review of integrating solar collectors to solar still, *Renew. Sustain. Energy Rev.*, 77 (2017) 1069–1097.
- [9] R.V. Singh, S. Kumar, M.M. Hasan, M.E. Khan, G.N. Tiwari, Performance of a solar still integrated with evacuated tube collector in natural mode, *Desalination*, 318 (2013) 25–33.
- [10] K. Sampathkumar, T.V. Arjunan, P. Senthilkumar, The experimental investigation of a solar still coupled with an evacuated tube collector, *Energy Sources, Part A*, 35 (2013) 261–270.
- [11] S. Kumar, A. Dubey, G.N. Tiwari, A solar still augmented with an evacuated tube collector in forced mode, *Desalination*, 347 (2014) 15–24.
- [12] H.J. Mosleh, S.J. Mamouri, M.B. Shafii, A.H. Sima, A new desalination system using a combination of heat pipe, evacuated tube and parabolic through collector, *Energy Convers. Manage.*, 99 (2015) 141–150.
- [13] M.B. Shafii, S.J. Mamouri, M.M. Lotfi, H.J. Mosleh, A modified solar desalination system using evacuated tube collector, *Desalination*, 396 (2016) 30–38.
- [14] S.W. Sharshir, G. Peng, N. Yang, M.A. Eltawil, M.K.A. Ali, A.E. Kabeel, A hybrid desalination system using humidification-dehumidification and solar stills integrated with evacuated solar water heater, *Energy Convers. Manage.*, 124 (2016) 287–296.
- [15] O. Bait, M. Si-Ameur, Tubular solar-energy collector integration: Performance enhancement of classical distillation unit, *Energy*, 141 (2017) 818–838.
- [16] O. Bait, Exergy, environ-economic and economic analyses of a tubular solar water heater assisted solar still, *J. Clean. Prod.*, 212 (2019) 630–646.
- [17] R.J. Issa, B. Chang, Performance study on evacuated tubular collector coupled solar still in west texas climate, *Int. J. Green Energy*, 14 (2017), DOI: 10.1080/15435075.2017.1328422
- [18] D.B. Singh, G.N. Tiwari, Energy, exergy and cost analyses of N identical evacuated tubular collectors integrated basin type solar stills: a comparative study, *Solar Energy*, 155 (2017) 829–846.
- [19] D.B. Singh, I.M. Al-Helal, Energy metrics analysis of N identical evacuated tubular collectors integrated double slope solar still, *Desalination*, 432 (2018) 10–22.
- [20] D.B. Singh, Improving the performance of single slope solar still by including N identical PVT collectors, *Appl. Thermal Eng.*, 131 (2018) 167–179.
- [21] D.B. Singh, Exergo-economic, enviro-economic and productivity analyses of N identical evacuated tubular collectors integrated double slope solar still, *Appl. Thermal Eng.*, 148 (2019) 96–104.
- [22] S.M. Elshamy, E.M.S. El-Said, Comparative study based on thermal, exergetic and economic analyses of a tubular solar still with semi-circular corrugated absorber, *J. Clean. Prod.*, 195 (2018) 328–339.
- [23] A.E. Kabeel, E.M.S. El-Said, Experimental study on a modified solar power driven hybrid desalination, *Desalination*, 443 (2018) 1–10.
- [24] A.E. Kabeel, E.M.S. El-Said, A hybrid solar desalination system of air humidification, dehumidification and water flashing evaporation: Part II. Experimental investigation, *Desalination*, 341 (2014) 50–60.
- [25] A.E. Kabeel, E.M.S. El-Said, A hybrid solar desalination system of air humidification dehumidification and water flashing evaporation: a comparison among different configurations, *Desalination*, 330 (2013) 79–89.
- [26] A.E. Kabeel, E.M.S. El-Said, Water production for irrigation and drinking needs in remote arid communities using closed-system greenhouse: a review, *Eng. Sci. Technol.*, 18 (2015) 294–301.
- [27] A.E. Kabeel, E.M.S. El-Said, Development strategies and solar thermal energy utilization for water desalination systems in remote regions: a review, *Desal. Wat. Treat.*, 52 (2014) 4053–4070.
- [28] A. E. Kabeel, E.M.S. El-Said, Technological aspects of advancement in low-capacity solar thermal desalination units, *Int. J. Sustain. Energy*, 32 (2013) 315–332.
- [29] R.K. Mishra, V. Garg, G.N. Tiwari, Energy matrices of U-shaped evacuated tubular collector (ETC) integrated with compound parabolic concentrator (CPC), *Solar Energy*, 153 (2017) 531–539.
- [30] D.B. Singh, G.N. Tiwari, Effect of energy matrices on life cycle cost analysis of partially covered photovoltaic compound parabolic concentrator collector active solar distillation system, *Desalination*, 397 (2016) 75–91.
- [31] P.I. Cooper, Digital simulation of experimental solar still data, *Sol Energy*, 14 (1973) 451.
- [32] R.V. Dunkle, Solar Water Distillation, the Roof Type Solar Still and Multi Effect Diffusion Still, *International Developments in Heat Transfer, A.S.M.E. Proceedings of International Heat Transfer, Part V, University of Colorado*, 1961, p. 895.
- [33] B.Y.H. Liu, R.C. Jordan, The interrelationship and characteristic distribution of direct, diffuse and total solar radiation, *Sol. Energy*, 4 (1960) 1–19.

Appendix-A

$$h_{\text{pf}} = 100 \text{Wm}^2 \text{K}^{-1} \quad (\text{A1})$$

$$h_{\text{rw}} = \left(0.82 \times 5.67 \times 10^{-8}\right) \left[\left(T_w + 273\right)^2 + \left(T_{\text{gi}} + 273\right)^2 \right] \left[T_w + T_{\text{gi}} + 546 \right]; \quad (\text{A2})$$

$$h_{\text{EW}} = 0.034 \times 5.67 \times 10^{-8} \left[\left(T_{\text{giE}} + 273\right)^2 + \left(T_{\text{giW}} + 273\right)^2 \right] \left[T_{\text{giE}} + T_{\text{giW}} + 546 \right] \quad (\text{A3})$$

$$E_1 = U_{cE} \left[h_{EW} + h_{1wW} \left(\frac{A_b}{2A_{gW}} \right) \right] A_{gE} A_{gW}; E_2 = U_{cW} [h_{EW} + U_{cE}] A_{gE} A_{gW}; \quad (A4)$$

$$E'_1 = U_{cW} \left[h_{EW} + h_{1wE} \left(\frac{A_b}{2A_{gE}} \right) \right] A_{gE} A_{gW}; E'_2 = U_{cE} [h_{EW} + U_{cW}] A_{gE} A_{gW}; \quad (A5)$$

$$H'_{22} = \left(\frac{2H}{A_b} \right) \left\{ U_b A_b + \left(\frac{1-K_k^N}{1-K_k} \right) (A_r F_r) U_L \right\}; \quad (A6)$$

$$H'_{11} = H_1 + H_2 + H_3 + H_4; H_1 = (U_{cE} A_{gE} + U_{cW} A_{gW}) \frac{A_b}{2} h_{1wE} h_{1wW}; \quad (A7)$$

$$H_2 = (h_{1wE} U_{cE} + h_{1wW} U_{cW}) h_{EW} A_{gE} A_g; H_3 = (h_{1wE} + h_{1wW}) U_{cE} U_{cW} A_{gE} A_g; \quad (A8)$$

$$H_4 = (h_{1wE} U_{cE} + h_{1wW} U_{cW}) h_{EW} A_{gE} A_g; \quad (A9)$$

$$K_{1E} = \alpha'_g h_{1wE} A_{gE} A_{gW} \left[h_{1wW} \left(\frac{A_b}{2A_{gW}} \right) + h_{EW} \left(1 + \frac{h_{1wW}}{h_{1wE}} \right) + U_{cW} \right]; \quad (A10)$$

$$K_{1W} = \alpha'_g h_{1wW} A_{gE} A_{gW} \left[h_{1wE} \left(\frac{A_b}{2A_{gE}} \right) + h_{EW} \left(1 + \frac{h_{1wE}}{h_{1wW}} \right) + U_{cE} \right]; \alpha_{wb} = (\alpha'_w + 2\alpha'_b h_1) H \quad (A11)$$

$$K'_{1E} = \alpha'_g h_{ewE} A_{gE} A_{gW} \left[h_{ewW} \left(\frac{A_b}{2A_{gW}} \right) + h_{EW} \left(1 + \frac{h_{ewW}}{h_{ewE}} \right) + U_{cW} \right]; \quad (A12)$$

$$K'_{1W} = \alpha'_g h_{ewW} A_{gE} A_{gW} \left[h_{ewE} \left(\frac{A_b}{2A_{gE}} \right) + h_{EW} \left(1 + \frac{h_{ewE}}{h_{ewW}} \right) + U_{cE} \right]; \quad (A13)$$

$$X_{11} = \frac{h_{ewE}(E_1 + E_2) + h_{ewW}(E'_1 + E'_2)}{H'_{11} + H'_{22}}; \quad F'_{1g} = \left(\frac{A_b}{H} \right) e^{-at}; \quad \alpha_{wb} = (\alpha'_w + 2\alpha'_b h_1) H \quad (A14)$$

$$Y_{11} = \left\{ (K_{1E} + \alpha_{wb}) I_{SE}(t) + (K_{1W} + \alpha_{wb}) I_{SW}(t) + \left(\frac{2H}{A_b} \right) (PF_1) (\alpha\tau)_{\text{eff}} \left(\frac{1-K_k^N}{1-K_k} \right) I_b(t) \right\} (e^{-at} - 1); \quad (A15)$$